

# Real-time inversion of polarization gate frequency-resolved optical gating spectrograms

Daniel J. Kane, Jeremy Weston, and Kai-Chien J. Chu

Frequency-resolved optical gating (FROG) is a technique used to measure the intensity and phase of ultrashort laser pulses through the optical construction of a spectrogram of the pulse. To obtain quantitative information about the pulse from its spectrogram, an iterative two-dimensional phase-retrieval algorithm must be used. Current algorithms are quite robust, but retrieval of all the pulse information can be slow. Previous real-time FROG trace inversion work focused on second-harmonic-generation FROG, which has an ambiguity in the direction of time, and required digital signal processors (DSPs). We develop a simplified real-time FROG device based on a single-shot geometry that no longer requires DSPs. We use it and apply the principal component generalized projections algorithm to invert polarization gate FROG traces at rates as high as 20 Hz. © 2003 Optical Society of America

*OCIS codes:* 320.0320, 320.7100, 320.7160.

## 1. Introduction

Measurement of ultrashort laser pulses is an important, yet often difficult, problem. One of several pulse-measurement techniques that has been developed is frequency-resolved optical gating (FROG).<sup>1–6</sup> In FROG a spectrogram of a pulse is formed optically by spectrally resolving the autocorrelation of the pulse to produce a plot of intensity versus frequency and time. The target information, the temporal and spectral profile of the input pulse (intensity and phase), can be obtained from the FROG trace by using two-dimensional phase-retrieval methods.<sup>7,8</sup>

While spectral phase interferometry for direct electric-field reconstruction (SPIDER) is a technique for direct pulse measurement that has been shown to be in real time, it is experimentally complex, requiring at least two embedded interferometers, a pulse stretcher, and a spectrometer. Furthermore it provides no feedback about the accuracy of the pulse reconstruction.<sup>9–11</sup> FROG, on the other hand, is experimentally simple, requiring only a spectrometer and an autocorrelator. It also provides a wealth of

information on the quality of pulse reconstruction,<sup>3</sup> and data acquisition can be rapid—less than 35 ms when a video camera and frame grabber are used. The resulting spectrogram provides immediate, qualitative information about the pulse. Depending on the required resolution, quantitative pulse characteristics generally require as many as a few minutes to obtain because of the iterative nature of the phase-retrieval calculation.

Consequently, real-time pulse measurement eluded FROG measurements until the development of a new FROG algorithm, principal components generalized projections (PCGP).<sup>4–6</sup> However, the application of the PCGP algorithm to the inversion of FROG traces was limited to blind-FROG inversions (the gate and pulse are independent)<sup>4,12</sup> until improvements to the PCGP algorithm allowed for FROG inversions (the gate is functionally related to the pulse).<sup>5</sup> While blind-FROG inversions can be made in real time, spectral constraints are necessary to ensure accurate retrievals, unnecessarily complicating the experimental apparatus and data collection.<sup>4</sup> While application of the PCGP algorithm to second-harmonic-generation (SHG) FROG is straightforward, applying the PCGP algorithm to other FROG geometries is more difficult because of algorithm instabilities. As a result, previous real-time FROG measurement systems have been limited to SHG FROG (which has a direction of time ambiguity).<sup>6</sup> In earlier publications a means was suggested for applying the PCGP algorithm to polarization-gate (PG) FROG geometries, but experimental verification was not done.<sup>6</sup>

---

D. J. Kane (djokane@swsciences.com) is with Southwest Sciences, Inc., Suite E-11, 1570 Pacheco Street, Santa Fe, New Mexico 87505. J. Weston and J. Chu are with Positive Light Inc., 101 Cooper Court, Los Gatos, California 95032.

Received 13 June 2002; revised manuscript received 18 October 2002.

0003-6935/03/061140-05\$15.00/0

© 2003 Optical Society of America

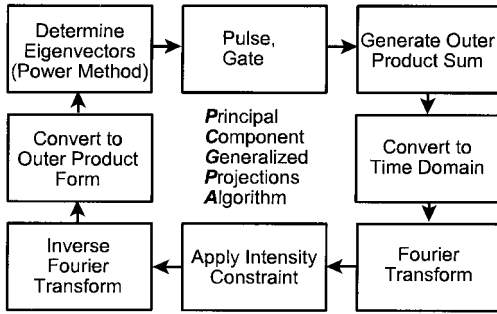


Fig. 1. Schematic of the PCGP algorithm.

In this paper we demonstrate for the first time, to our knowledge, the application of the PCGP polarization-gate (PG) FROG algorithm to real-time inversion of PG FROG traces. We also demonstrate for the first time, to our knowledge, that near noise-limited convergence can be achieved in real-time FROG trace inversions.<sup>13</sup> In addition, we simplify real-time FROG devices by eliminating the need for digital signal processors (DSPs) and by using a single-shot geometry rather than the previous multishot geometry. Some optimizations that can be implemented to improve the performance of real-time FROG systems are also discussed. First, we review the PCGP phase-retrieval algorithm and apply it to the inversion of PG FROG traces. We then discuss the optical experimental hardware. Finally, the software operation is described along with the experimental results.

## 2. Algorithm of the Principal Components Generalized Projection

The PCGP algorithm (Fig. 1) is a generalized projections algorithm<sup>14–16</sup> that is not encumbered by a minimization step. It is based on the idea that any FROG trace, spectrogram, or sonogram<sup>17–21</sup> can be constructed from the outer product of two complex vectors representing the pulse and the gate. Construction of the new guess for the pulse and gate is reduced to an eigenvector calculation.<sup>4–6</sup> A simple rearrangement of the outer product matrix elements produces the time-domain FROG trace. Fourier transforming the matrix columns converts the time-domain FROG trace into the frequency domain. Because all these steps are reversible, one can subsequently estimate the pulse efficiently by multiplying the previous estimate for the pulse (or gate) by the new outer product form matrix by using

$$\begin{aligned} \text{probe}_i^{(n+1)} &= O^{ij} O^{ji*} \text{probe}_j^{(n)}, \\ \text{gate}_i^{(n+1)} &= O^{ji*} O^{ij} \text{gate}_j^{(n)}, \end{aligned} \quad (1)$$

where  $O$  is the outer product form matrix, probe is the pulse to be measured, gate is the gate, and superscript  $n$  is the iteration. The algorithm is robust, converging from an initial guess of random noise in 20–40 iterations for most FROG traces, and can be efficiently coded to iterate quickly on computers.

By nature the PCGP algorithm is a blind-FROG

algorithm because no assumptions are made about the functional dependence between the probe and the gate, which may result in some inaccuracies.<sup>4</sup> Summing two outer products can alleviate these inaccuracies by applying an additional constraint on the algorithm<sup>6</sup>:

$$O^{ij} = \text{probe}_i^j \text{gate}_j^i + \Gamma^{-1} (\text{gate}_i^j \Gamma (\text{probe}_j^i)), \quad (2)$$

where  $O$  is the outer product, probe is the pulse to be measured, gate is the gate pulse,  $\Gamma$  is a function that converts the pulse to the gate (providing the additional mathematical form constraint), and  $\Gamma^{-1}$  is its inverse that converts the gate back to the probe. For SHG FROG the inverse is trivial; the probe and the gate are equal. Consequently this version of the PCGP algorithm has been successfully used to invert SHG FROG traces in real time.<sup>5</sup>

In the PG FROG case,  $\Gamma$  has no inverse. Thus a pseudoinverse is constructed from the square root of the gate and the phase of the probe. Because the pseudoinverse is equal to the pulse when the algorithm is converged, this constructed inverse has no effect on the accuracy of the inversion. However, in PG FROG inversion, the square-root function in the pseudoinverse can cause a spurious signal in the wings, resulting in algorithm instabilities. Applying Eq. (2) on alternate iterations of the algorithm (by using only the outer product on the other iterations) results in better stability, but this has never been demonstrated for real-time inversions or for experimental data.<sup>6</sup> Because real-time FROG systems require that the previous result be used as the initial guess for the next iteration, algorithm instabilities can cause a real-time FROG system to be unstable and unable to track pulse changes. In this work we found that, when using the symmetrization with the pseudoinverse on every other iteration, the algorithm inverted pulses with low error (noise-limited convergence) and it was stable, successfully tracking real-time changes in pulse compressor settings.

As a cross-check for the retrieval, the intensity of the retrieved pulse can be compared with the retrieved gate. For the best retrievals the intensity of the retrieved pulse should be identical to the retrieved gate. While slight differences between the retrieved pulse intensity and the retrieved gate are little cause for alarm, very poor calibrations or large, nonuniform backgrounds in the FROG trace cause large discrepancies between the retrieved gate and the retrieved pulse intensity, warning the user of an inaccurate retrieval.

## 3. Experiment and Analysis

Output pulses from Positive Light's Hurricane chirped-pulse regenerative amplifier were measured with Positive Light's single-shot PG FROG device. A stretcher/compressor integral to the regenerative amplifier allows a variation of the input-pulse characteristics. Shown in Fig. 2 is a schematic diagram of a single-shot PG FROG device. The input beam to the FROG device is split into two replicas, the probe

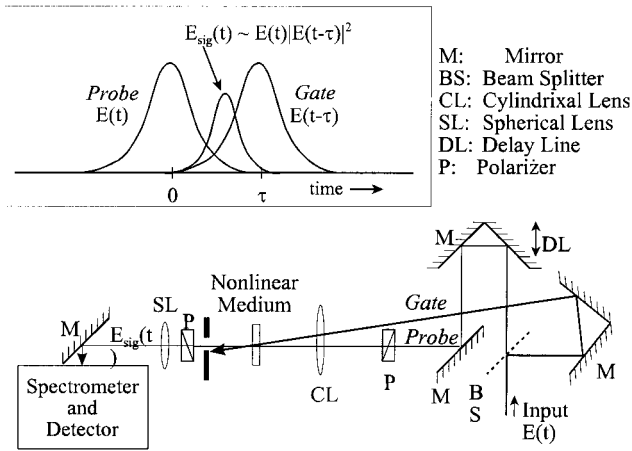


Fig. 2. Schematic diagram of a single-shot PG FROG device. The input pulse is split into two replicas, the pulse and the gate, that cross at an angle to map the time delay to a spatial coordinate. A cylindrical lens focuses the gate and probe into the nonlinear medium (quartz). A polarizer is used to set the polarization of the probe to 45 deg relative to the gate. The gate pulse induces birefringence in the nonlinear medium, rotating the polarization of the probe. The signal leaks through the second polarizer, set at 90 deg relative to the first, and is spectrally resolved with an imaging spectrometer. The inset shows the signal pulse's functional relationship to the probe and the gate pulses.

and the gate. The probe beam is sent through a high-quality calcite polarizer (~55-dB rejection) that sets the polarization of the probe at 45 deg relative to the gate. Both beams are focused with a cylindrical lens into a nonlinear medium (quartz window). The probe and gate beams are set to propagate at an angle to map the delay between the two beams onto a spatial coordinate as they intersect in the nonlinear medium.

The gate induces birefringence in the quartz that follows the intensity profile of the gate by the instantaneous optical Kerr effect. Thus at regions in the nonlinear material where the gate spatially and temporally overlaps with the probe pulse the probe pulse's polarization is rotated slightly. To block the portions of the probe that are not rotated, the probe beam is sent through another polarizer that is set 90 deg relative to the first polarizer. Only rotated portions of the probe (where the pulse and gate overlap in space and time) pass through the second polarizer. This leakage (signal) is spectrally resolved in an imaging spectrometer.

The FROG trace (intensity versus time and frequency) formed at the focal plane of the imaging spectrometer is recorded by a video camera. Before the FROG trace is sent to the algorithm, the square root of the FROG trace must be taken. Because only an 8-bit analog-to-digital converter is used in the frame grabber to digitize the video signal, computing the square root effectively reduces the dynamic range of the FROG trace from 256 to 16. Such a reduction in dynamic range greatly increases the deleterious effect background in the FROG trace has on pulse reconstruction. To improve the reconstruction of the

retrieved pulse, an analog computation of the square root of the intensity is completed before digitization by setting the gamma of the video camera as close to 0.5 as possible. When this is done, a dynamic range of 256 is preserved for the algorithm.

Although an expensive DSP system was used for data collection and inversion of real-time SHG FROG traces in the past, for this work we simplify the data-acquisition system and computational hardware. The frame grabber, residing in a 550-MHz dual Pentium III computer (Windows NT operating system), captures FROG traces at ~20 frames/s. The raw video is displayed at roughly 18 frames/s (slightly slower than the capture rate) with a resolution of 640 × 480 pixels. A selected number of frames (typically one) are resampled and averaged.

Raw video frames read from the frame grabber are resampled to the proper relationship between the time and frequency axis:  $1/\Delta f = N\Delta t$ , where  $\Delta f$  is the frequency spacing of the frequency axis of the FROG trace,  $N$  is the number of pixels, and  $\Delta t$  is the time spacing.<sup>3</sup> Although choices of either  $\Delta t$  or  $\Delta f$  (but not both) can be arbitrary, to prevent undersampling or oversampling of the experimental FROG trace in either the frequency or time direction,  $\Delta t$  and  $\Delta f$  are found with

$$\Delta t = \left( \frac{N_t}{N_f \Delta f} \right)^{1/2}, \quad (3)$$

$$\Delta f = \frac{1}{N_{\text{resampled}} \Delta t},$$

where  $N_t$  is the number of time points in the raw FROG trace,  $N_f$  is the number of frequency points in the raw FROG trace, and  $N_{\text{resampled}}$  is the number of time and frequency points in the resampled FROG trace. If the resampled FROG trace does not have enough points along the time and/or frequency axis, it is zero padded before being averaged.

After averaging is complete, the resampled FROG trace is detrended by setting the average of the FROG trace background to zero and by removing any slope on the background; negative intensities are kept to suppress spurious noise in the wings of the retrieved pulse. Depending on the trade-off between noise rejection required and the pulse update rate, the number of resampled FROG traces summed (averaged) can be varied; for maximum speed, no FROG traces are averaged.

The resampled FROG trace is sent to the PG PCGP algorithm for inversion. The inversion algorithm is a separate process (thread) running concurrently with the data-acquisition process at ~160–200 iterations/s. Immediately before a new FROG trace is sent to the inversion engine an updated pulse is retrieved from the algorithm and displayed. To reduce the computational requirements on the algorithm, the previous result from the PG PCGP algorithm is used as the initial guess for the next inversion. As a result the 20–40 iterations required for full convergence of the algorithm

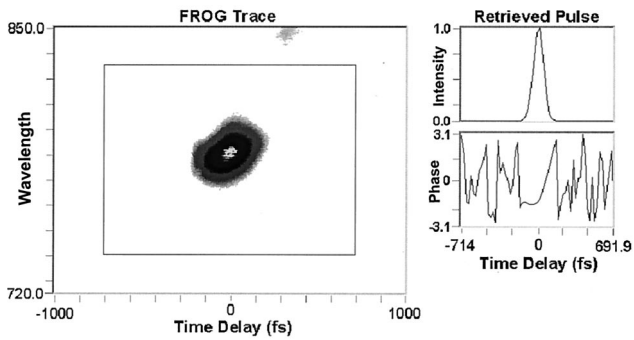


Fig. 3. Screen data from the real-time FROG program. The large plot on the left side is the raw spectrogram directly from the video camera. The square around the spectrogram indicates the portion of the raw FROG trace used for the pulse retrieval. The plots on the right show the retrieved pulse intensity and phase. The FWHM of the pulse is 98.9 fs and the bandwidth is 5.37 THz. The actual retrieval rate was 19.4 retrievals/s with eight iterations of the algorithm between updates.

are not necessary; the approximately eight iterations of the algorithm between each update are enough to allow tracking of changes in the pulse intensity and phase.

Figure 3 shows screen data from the real-time FROG inversion program. The large display on the left is the captured raw video containing the FROG trace. The raw data are displayed as fast as possible but usually lag behind the capture rate. Two plots

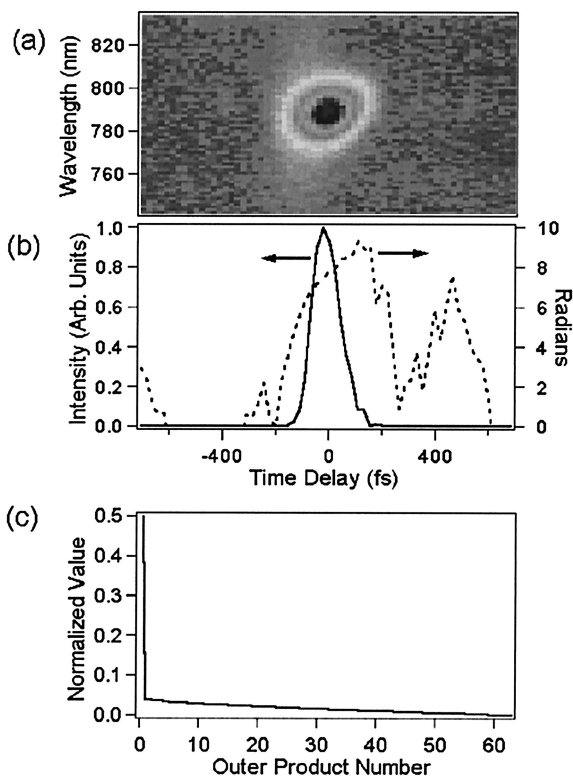


Fig. 4. Example of retrieved data: (a) resampled FROG trace; (b) intensity and phase of the retrieved pulse; (c) weights. The nearly straight line indicates close to noise-limited convergence.

on the right show the pulse intensity (top) and the pulse phase (bottom).

Figure 4 shows an example of retrieved data from the FROG device. Figure 4(a) shows the resampled FROG trace that is sent to the PG PCGP algorithm. Figure 4(b) shows a plot of the retrieved pulse intensity and phase. Figure 4(c) shows a singular value decomposition<sup>22</sup> weight plot.<sup>13</sup> The straight line indicates noise-limited convergence. The FROG trace error was  $\sim 1\%$  and the retrieved pulse and gate were nearly identical, indicating that the background in the FROG trace had minimal effect on the retrieval.

#### 4. Conclusions

In conclusion, we have applied the PCGP algorithm to the real-time inversion of PG FROG traces for the first time, to our knowledge, and demonstrated the ability to obtain near noise-limited convergence of FROG inversions in real time. Moreover, we remove the need for DSP's in real-time FROG devices together with simplifying the acquisition hardware by moving to a single-shot geometry.

This material is based upon work supported by the National Science Foundation under grant 9801116. D. J. Kane acknowledges the help of J. Denson.

#### References

1. D. J. Kane and R. Trebino, "Characterization of arbitrary femtosecond pulses using frequency-resolved optical gating," *IEEE J. Quantum Electron.* **29**, 571–579 (1993).
2. D. J. Kane, and R. Trebino, "Single-shot measurement of the intensity and phase of an arbitrary ultrashort pulse by using frequency-resolved optical gating," *Opt. Lett.* **18**, 823–825 (1993).
3. R. Trebino, K. W. DeLong, D. N. Fittinghoff, J. N. Sweetser, M. A. Krumbügel, B. A. Richman, and D. J. Kane, "Measuring ultrashort laser pulses in the time-frequency domain using frequency-resolved optical gating," *Rev. Sci. Instrum.* **68**, 3277–3295 (1997).
4. D. J. Kane, G. Rodriguez, A. J. Taylor, and T. S. Clement, "Simultaneous measurement of two ultrashort laser pulses from a single spectrogram in a single shot," *J. Opt. Soc. Am.* **14**, 935–943 (1997).
5. D. J. Kane, "Real-time measurement of ultrashort laser pulses using principal component generalized projections," *IEEE J. Sel. Top. Quantum Electron.* **4**, 278–284 (1998).
6. D. J. Kane, "Recent progress toward real-time measurement of ultrashort laser pulses," *IEEE J. Quantum Electron.* **35**, 421–431 (1999).
7. R. Trebino and D. J. Kane, "Using phase retrieval to measure the intensity and phase of ultrashort laser pulses: frequency-resolved optical gating," *J. Opt. Soc. Am. A* **10**, 1101–1111 (1993).
8. J. R. Fienup, "Reconstruction of a complex-valued object from the modulus of its Fourier transform using a support constraint," *J. Opt. Soc. Am. A* **4**, 118–123 (1987).
9. T. M. Shuman, M. E. Anderson, J. Bromage, C. Iaconis, L. Waxer, and I. A. Walmsley, "Real-time SPIDER: ultrashort pulse characterization at 20 Hz," *Opt. Express* **5**, 134–143 (1999).
10. L. Gallmann, D. H. Sutter, N. Matuschek, G. Steinmeyer, U. Keller, C. Iaconis, and I. A. Walmsley, "Characterization of sub-6-fs optical pulses with spectral phase interferometry for direct electric-field reconstruction," *Opt. Lett.* **24**, 1314–1316 (1999).
11. C. Iaconis, V. Wong, and I. A. Walmsley, "Direct interferomet-

- ric techniques for characterizing ultrashort optical pulses," *IEEE J. Sel. Top. Quantum Electron.* **4**, 285–294 (1998).
12. C. W. Siders, A. J. Taylor, and M. C. Downer, "Multipulse interferometric frequency-resolved optical gating: real-time phase-sensitive imaging of ultrafast dynamics," *Opt. Lett.* **22**, 624–626 (1997).
  13. D. J. Kane, F. G. Omenetto, and A. J. Taylor, "Convergence test for inversion of frequency-resolved optical gating spectrograms," *Opt. Lett.* **25**, 1216–1218 (2000).
  14. E. Yudilevich, A. Levi, G. J. Habetler, and H. Stark, "Restoration of signals from their signed Fourier-transform magnitude by the method of generalized projections," *J. Opt. Soc. Am. A* **4**, 236–246 (1987).
  15. A. Levi and H. Stark, "Image restoration by the method of generalized projections with applications to restoration from magnitude," *J. Opt. Soc. Am. A* **1**, 932–943 (1984).
  16. W. H. Press, S. A. Teukolsky, W. T. Vetterling, and B. P. Flannery, *Numerical Recipes in C: The Art of Scientific Computing*, 2nd ed. (Cambridge University, Cambridge, England, 1995).
  17. D. T. Reid, "Algorithm for complete and rapid retrieval of ultrashort pulse amplitude and phase from a sonogram," *IEEE J. Quantum Electron.* **35**, 1584–1589 (1999).
  18. J. L. A. Chilla and O. E. Martinez, "Direct determination of the amplitude and phase of femtosecond light pulses," *Opt. Lett.* **16**, 39–41 (1991).
  19. E. B. Treacy, "Measurement and interpretation of dynamic spectrograms of picosecond light pulses," *J. Appl. Phys.* **42**, 3848–3858 (1971).
  20. L. Cohen, "Time-frequency distributions—a review," *Proc. IEEE* **77**, 941–981 (1989).
  21. V. Wong and I. A. Walmsley, "Ultrashort-pulse characterization from dynamic spectrograms by iterative phase retrieval," *J. Opt. Soc. Am. B* **14**, 944–949 (1997).
  22. A. K. Jain, *Fundamentals of Digital Image Processing*, 1st ed. (Prentice-Hall, Englewood Cliffs, N.J., 1989).